

COUPLING CHARACTERISTICS OF MESO-STRUCTURE AND THERMOPHYSICAL PARAMETERS OF DEEP GRANITE UNDER HIGH GEO-TEMPERATURE

by

**Huan WANG^{a,b}, Shuang YOU^{a,b*}, Hong-Guang JI^{a,b},
Hui-Ci XU^{a,b}, Qi LI^{a,b}, and Hu-Zhen LI^{a,b}**

^a School of Civil and Resource Engineering,
University of Science and Technology, Beijing, China

^b Beijing Key Laboratory of Urban Underground Space Engineering, USTB, Beijing, China

Original scientific paper
<https://doi.org/10.2298/TSCI2106621W>

Polarizing microscope, nuclear magnetic resonance, and thermal constant analyzer were used to test the granite samples in the depth of 1500-2000 m in San-shandao before and after the heat treatment and be carried out to study the corresponding relationship between rock meso-structure characteristics and different geothermal temperature circumstances, and the influence of thermal cycling on rock meso-structure. Tests results present that the porosity, pore size distribution, thermal conductivity and specific heat capacity are significantly affected by the environment where the rock occurs, mineral composition and particle size, and the increase in porosity and water content will cause the thermal conductivity and specific heat capacity to decrease.

Key words: *deep granite, geo-temperature, meso-structure, thermal properties, laboratory test*

Introduction

With the gradual decrease of shallow resources, deep mining is the inevitable trend of global mining development in the future [1]. The rock in deep strata is in high temperature, so the meso-structure and thermophysical parameters have variability compared with the shallow rock [2-5]. Therefore, it is of great significance for the stability of rock mass engineering to study the evolution characteristics of meso-structure and thermophysical parameters of deep rock under the high geo-temperature. Nasseri *et al.* [6] studied the main factors of mineral particle cracking under high temperature environment. Gan *et al.* [7] found thermal cycling causes the crack density of granite to increase, resulting in the cracking of the rock structure. For the granite subjected to more thermal cycles, the rock cracking is more severe. Zhou *et al.* [8] found that the damage to the micro-structure of granite caused by high temperature is a physical change rather than a chemical change. Wang *et al.* [9] concluded that repeated heating and cooling cycles would only cause minor damage to the rock. Avanthi *et al.* [10] analyzed the porosity and pore connectivity of the rock after heat treatment. Gautam *et al.* [11, 12] found that high temperature gradually reduces the thermal conductivity and thermal diffusivity of granite, and pointed out that the formation and growth of micro-cracks are related to thermal conductivity and thermal diffusion.

* Corresponding author, e-mail: youshuang@ustb.edu.cn

When studying the influence of temperature on the meso-structure of rocks, most of the predecessors used SEM and polarizing microscope [13, 14]. They could only observe the local characteristics of the sample, but could not obtain a complete spatial distribution law. Some scholars used nuclear magnetic resonance (NMR) to study the thermal damage mechanism of rocks to make up for such shortcomings [15-19]. However, when they used this technology to study the porosity, meso-structure and permeability of rocks, they only studied the damage degree of temperature on the meso-structure of rocks, and have little research on how temperature affects the evolution law and fracture mode of rock meso-structure.

In this paper, the polarizing microscope, NMR, and thermal constant analyzer were used to test the meso-structure and thermal properties of granite from the depth of 1500-2000 m in Sanshandao. There was a discussion on the pore connectivity, the evolution of meso-pores and pore size distribution, and the micro-crack propagation mode in deep granite. The coupling relationship among rock meso-structure characteristics, geothermal temperature, and the thermal cycling on rock meso-structure were analyzed. The results would provide a reference for studying the evolution characteristics of the meso-structure and the influencing factors of thermophysical parameters under the high geo-temperature.

Experimental procedure and sample preparation

The field tests were carried out in Sanshandao, Shandong province. Temperature was measured in the depth of 1500-2000 m and the maximum temperature is close to 55~60 °C. The granite samples were prepared into $\varnothing 50 \text{ mm} \times 25 \text{ mm}$, fig. 1. The experiment was carried out according to the three steps:

- The rocks at different depths were made into thin slices and the polarizing microscope was used to observe their mineral composition, form and particle size.
- The samples were tested to measure the porosity, pore size distribution, thermal conductivity, and specific heat capacity of granite by NMR and thermal constant analyzer at 20 °C.
- Putting the specimens into heating device, and then the temperature was increased to 60 °C by 2 °C per minute, keeping the temperature for two hours and natural cooling to the 20 °C in the heating device, after which specimens were subjected to thermal constant experiments, NMR and water saturation experiments. The thermal cycling tests were repeated until the pore diameter curve did not change or was less than 0.01 mm. The test process and equipment are shown in fig. 1.



Figure 1. Test procedures and equipment

Meso-structure characteristics of deep granite

Meso-structure of deep granite

From fig. 2 and tab. 1, the 1500 m and 1600 m samples have larger particle sizes (1.2~7.5 mm), and there are traces of opaque substances between different crystals. The 1700 m sample has a wide particle size distribution, and the potash feldspar and plagioclase

are clayization seriously. The particle sizes of the 1800 m, 1900 m, and 2000 m specimens are about 0.8-5.5 mm, the inter-embedding between different crystals and the boundaries are obvious. There is no distinct difference in mineral composition except for 1700 m specimen, about 40% of which is oblique feldspar, about 25% of which is potassium feldspar and quartz, and about 6% of which is black mica, chlorite and other minerals.

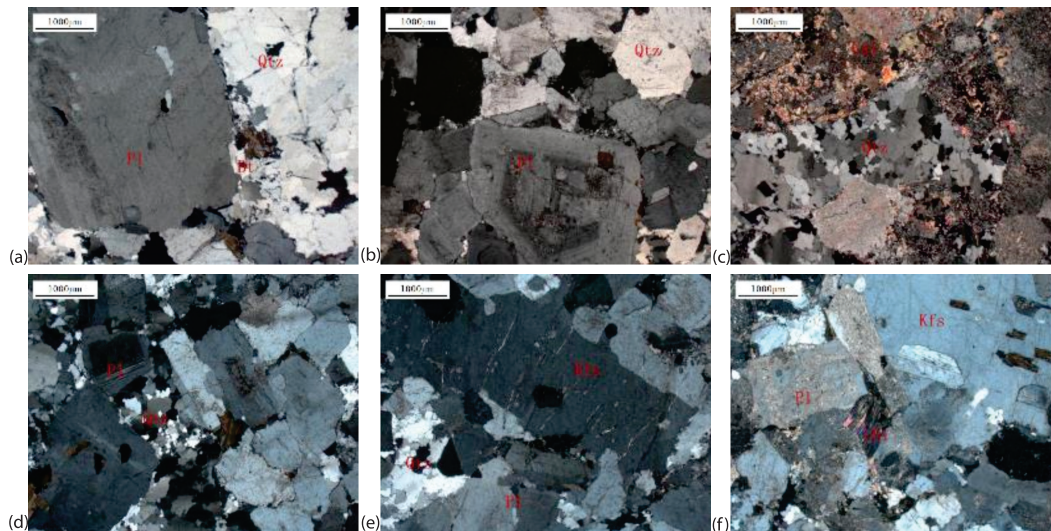


Figure 2. Granit meso-structure with depth; (a) 1500 m, (b) 1600 m, (c) 1700 m, (d) 1800 m, (e) 1900 m, and (f) 2000 m

Table 1. The mineral composition of rocks

Depth [m]	Types	Particle size [mm]	Potash feldspar	Plagioclase	Quartz	Others
1500	Biotite monzonitic granite	2~7	23% crystal size >10mm	37%	33%	Biotite, chlorite: 7%
1600	Biotite monzonitic granite	1.2~7.5	23% crystal size >10mm	41%	30%	Biotite, chlorite: 7%
1700	Sericitized granite	1~7	28% Clayization	42% Clayization	24%	Muscovite, calcite: 6%
1800	Biotite monzonitic granite	0.8~5.5 (Medium grain)	24%	43%	25%	Biotite, chlorite: 8%
1900	Biotite monzonitic granite	0.9~5.2 (Medium grain)	29%	38%	26%	Biotite, chlorite: 7%
2000	Biotite monzonitic granite	1.3~5.5 (Medium grain)	28%	36%	32%	Biotite, chlorite: 4%

Pore distribution of deep granite

In order to quantitatively describe the pore size, the pore size below $0.1\ \mu\text{m}$ is defined as the small pore, $0.1\sim 1\ \mu\text{m}$ as the medium pore, and more than $1\ \mu\text{m}$ as the large pore. The pore size distribution is shown in fig. 3. The 1500 m and 1600 m specimens belong to the single-peak shape, indicating that the specimens are mainly of large pore size, which has a single pore type, good pore size sorting, and pore connectivity. The 1700 m specimen has left-high-right-low double-peak shape, with the peak appearing near $0.1\ \mu\text{m}$, indicating that the specimen mainly has small pore and fewer large pore, which is mainly due to the serious clayization of the rock, which causes more internal fissures in the rock, moreover, some clay fills the large pore, resulting in an increase in the proportion of small pores. The 1800 m and 1900 m specimens show a right-high-left-low shape, which is typical of dense granites, the second peak is about twice as high as the first peak, and the double-peak structure is obvious. It is presumed that most of the independent pore connectivity between small and large pore is poor. The 2000 m specimen shows a three-peak shape, the peak values are almost same and the curve distribution is wide, those indicate the pore connectivity is low.

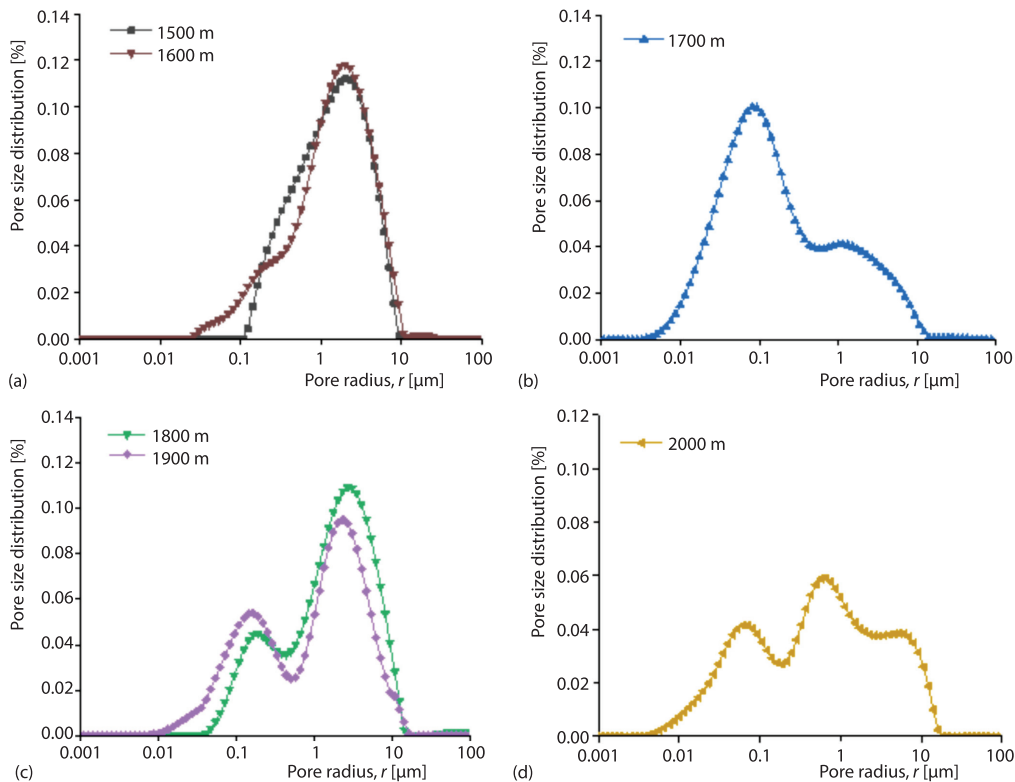


Figure 3. Pore size distribution with depth; (a) single-peak shape, (b) left-high-right-low double-peak shape, (c) right-high-left-low shape, and (d) three-peak shape

The three groups of rock samples of 1800 m, 1900 m, and 2000 m were taken to draw the cumulative pore radius proportion diagram, fig. 4, found that the starting point of the curve moves to the left and the slope of the curve decreases with the increase of the depth of the sample. It is concluded that with the increase of the depth of rock, the radius of the pore is smaller

and the proportion of the small pore is increasing. Figure 5 shows a histogram of cumulative pore radius at different depths. The 1800 m specimen mainly have large pore, accounting for about 65% and less than 5% of small pore. The 1900 m specimen has the same characteristics, but the proportion difference of cumulative pore radius decreases slightly and the proportion of small pore in the rock increases and the proportion of large pore decreases. The 2000 m specimens have a uniform distribution in each pore size range. In general, as the rock depth increases, the proportion of small holes increases significantly, the proportion of medium pore increases less, and the proportion of large pore.

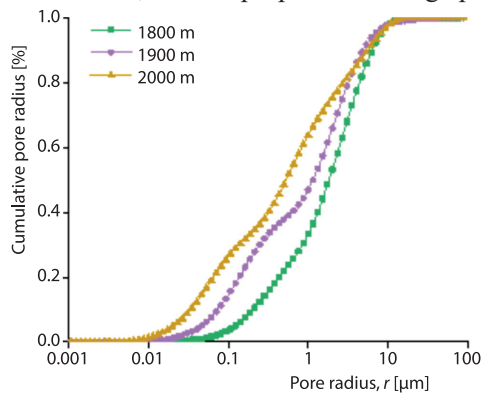


Figure 4. Cumulative pore radius curve

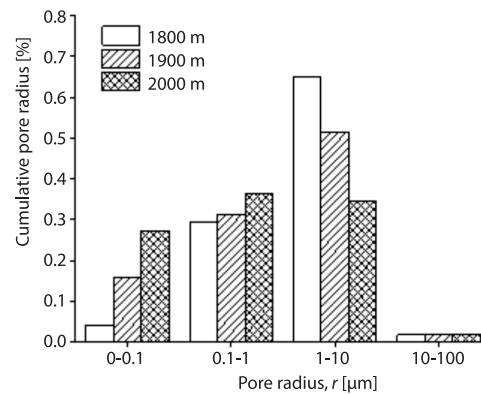


Figure 5. Cumulative pore radius histogram

Thermophysical characteristics of deep granite under geo-temperature

Thermal conductivity and specific heat capacity of deep rocks

Transient plane source is the most accurate method to study heat transfer properties. The resistance change of the probe can be expressed by:

$$R_{(t)} = R_0[1 + a\Delta T_i + a\Delta T_{(T)}] \quad (1)$$

where $R_{(t)}$ is resistance of probe before instant recording, a – the temperature coefficient of resistance, ΔT_i – the temperature difference in the film protective layer, and $\Delta T_{(T)}$ – the average temperature rise of the probe when it is in perfect contact with the sample.

Here, $\Delta T_{(T)}$ can be expressed:

$$\Delta T_{(T)} = \frac{QD_{(T)}}{\lambda R_0 \sqrt{\pi^3}} \quad (2)$$

where Q is constant output power, R_0 – the probe radius, λ – the thermal conductivity of the tested sample, and $D_{(T)}$ – the time function.

Assume that:

$$R^* = R_0(1 + \alpha\Delta T_i), \quad K = \frac{aR_0Q}{\lambda R_0 \sqrt{\pi^3}} \quad (3)$$

Substituting eq. (2) into eq. (1) yields:

$$R_{(T)} = R^* + KD_{(T)} \quad (4)$$

where $R_{(T)}$ is the measured resistance.

The thermophysical parameters are measured at 20 °C is shown in figs. 6 and 7. The thermal conductivity shows an increasing trend with the increase of rock depth, but at 1700 m, the thermal conductivity has a very large increment, which is related to the serious clayization of the sample. The clay is present in the pores between the particles and acts as a heat-conducting medium that connects the particles, which improve the thermal conductivity of rock. The specific heat capacity also shows an increasing trend with the increase of rock depth, the specific heat capacity of the sample increased abruptly at 1600 m. According to the pore size distribution, the proportion of the small pores of the 1500 m, 1800 m, 1600 m, 1900 m, and 2000 m specimens increases, which is similar to the law of specific heat capacity. This means that the larger the proportion of small holes in the rock, the greater the specific heat capacity.

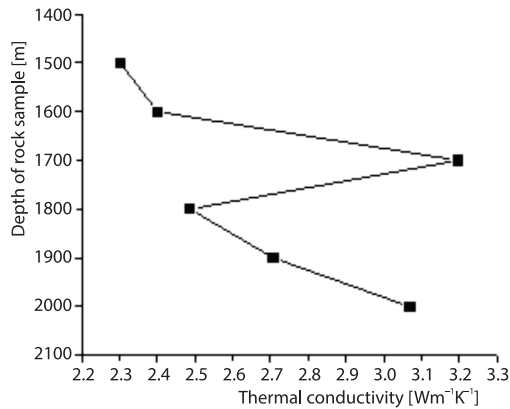


Figure 6. Thermal conductivity with depth

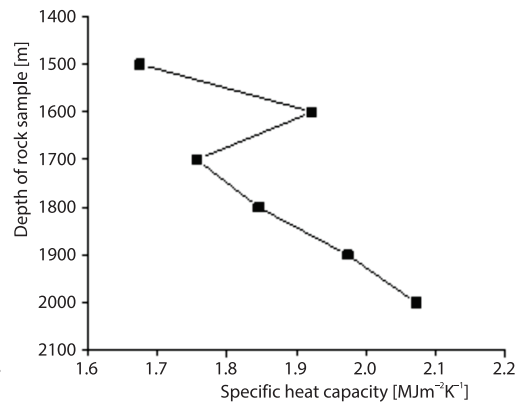


Figure 7. Specific heat capacity with depth

Effect of porosity and water content on thermal conductivity and specific heat capacity

Figure 8 shows the distribution of changes of rock porosity and thermal conductivity and specific heat capacity under dry conditions. It can be concluded that the thermal conductivity and specific heat capacity decrease with the increase of porosity, and the rate of decline becomes faster with the increase of porosity. This is principally because the thermal conductivity of the air is much lower than that of the mineral particles, when the porosity of rock increases, air will enter into the pores, which will reduce the heat transfer performance between

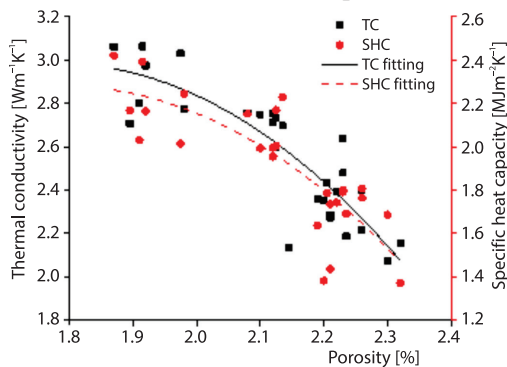


Figure 8. Thermal conductivity (TC) with porosity

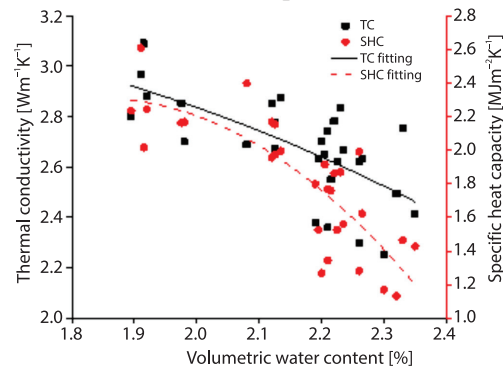


Figure 9. Specific heat capacity (SHC) with water content

the mineral particles, leading to the decrease of the thermal conductivity of rock. As shown in fig. 9, the change of water content has a significant impact on the thermophysical parameters, that is, as the rock water content increases, the thermal conductivity and specific heat capacity coefficient decreases, and the rate of decrease in specific heat capacity is greater than the thermal conductivity.

The influence of thermal cycling on pore size distribution

Figure 10 shows the pore size distribution of rock under thermal cycling. According to the curve, it can be concluded that the first heating cycle has the greatest effect on the pore size distribution curve of the granite. After thermal cycling, the proportion of small pore increases and the peak value of large pore decreases, which is because high temperatures can cause damage to the rock, resulting in the development of fissures, and some minerals are broken after the volume increases to a certain extent under the joint action of temperature and water, and the collapsed minerals fill part of the pores. This studies also support the aforementioned conclusion, proving that 60 °C can cause damage to the internal structure of rocks and the first heating has the greatest impact on the meso-structure of rocks, while the thermal cycling only slightly damages the rocks.

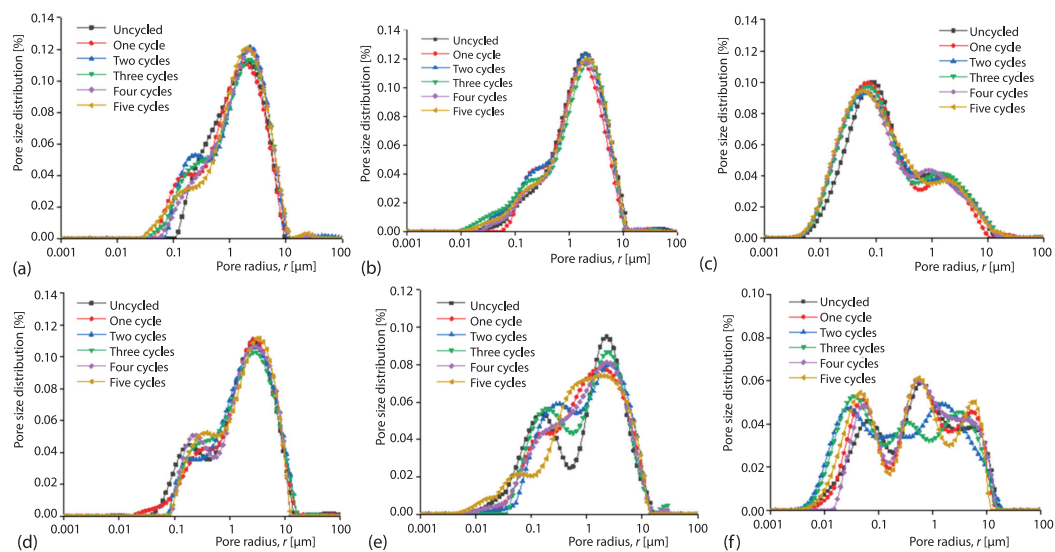


Figure 10. Pore size distribution of granite samples under thermal cycling at different depth; (a) 1500 m, (b) 1600 m, (c) 1700 m, (d) 1800 m, (e) 1900 m, and (f) 2000 m

Conclusion

As the depth increases, the mineral particle structure become complexity, the porosity of the rock decrease, the proportion of small pore ($r < 0.1 \mu\text{m}$) increases significantly and the proportion of large pore ($r > 0.1 \mu\text{m}$) decreases, the thermal conductivity and specific heat capacity show an increasing trend. The increase of porosity and water content will cause the thermal conductivity and specific heat capacity to decrease. Porosity has a greater effect on thermal conductivity and less on heat capacity compared to water content. The clayization of rock will cause the thermal conductivity to increase and the number of small holes will in-

duce the specific heat capacity to increase. Under the thermal cycling from 60-20 °C, the pore ($r > 0.1 \mu\text{m}$) developing, which enhances meso fissures connectivity in the granite. Especially, the meso-structure of the rock significantly affected in the first cycle of heating at 60 °C, which indicate the thermal cycling has effect on rock inner parts.

Acknowledgment

This work was supported by the State Key Research Development Program of China (Grant No. 2016YFC0600801), National Natural Science Foundation of China (Grant No. 51774021 and No. 52074021), Key Research Development Program of Shandong Province (2019SDZY05) and the Fundamental Research Funds for the Central University (FRF-GF-20-01B).

Nomenclature

a – temperature coefficient of resistance, [–]	$R_{(t)}$ – resistance of probe, Ω
K – scale factor, [–]	ΔT_i – temperature difference, [K]
Q – constant output power, [W]	t – time, [s]

References

- [1] Teng, J. W., et al., Analysis of Chinese Coal Demand, Exploration Potential and Efficient Utilization, *Chinese Journal of Geophysics*, 59 (2016), 12, pp. 4633-4653
- [2] Xie, H. P., et al., Research and Exploration of Deep Rock Mass Mechanics, *Chinese Journal of Rock Mechanics and Engineering*, 34 (2015), 11, pp. 6-23
- [3] Peng, K., et al., Evolutionary Characteristics of Mode-I Fracture Toughness and Fracture Energy in Granite from Different Burial Depths under High-Temperature Effect, *Engineering Fracture Mechanics*, 239 (2020), 7, ID107306
- [4] Gao, M. Z., et al., Principle and Technology of Coring with in-situ Pressure and Gas maintaining in Deep Coal Mine, *Journal of China Coal Society*, 46 (2021), 3, pp. 885-897
- [5] Xie, H. P., et al., Several Disruptive Technical Ideas and Research Directions in the Field of Deep Science, *Advanced Engineering Sciences*, 49 (2017), 1, pp. 1-8
- [6] Nasser, M. H. B., et al., Coupled Evolution of Fracture Toughness and Elastic Wave Velocities at High Crack Density in Thermally Treated Westerly Granite, *International Journal of Rock Mechanics and Mining Sciences*, 44 (2007), 5, pp. 601-616
- [7] Gan, F., et al., Effect of Thermal Cycling-Dependent Cracks on Physical and Mechanical Properties of Granite for Enhanced Geothermal System, *International Journal of Rock Mechanics and Mining Sciences*, 134 (2020), 5, ID104476
- [8] Zhou, X. P., et al., Real-Time Experiment Investigations on the Coupled Thermomechanical and Cracking Behaviors in Granite Containing Three Pre-Existing Fissures, *Engineering Fracture Mechanics*, 224 (2020), 4, ID106797
- [9] Wang, F., et al., Influence of Repeated Heating on Physical-Mechanical Properties and Damage Evolution of Granite, *International Journal of Rock Mechanics and Mining Sciences*, 136 (2020), 5, ID104514
- [10] Avanthi, B. L. I., et al., Quantification of Thermally-induced Microcracks in Granite Using X-ray CT Imaging and Analysis, *Geothermics*, 81 (2019), 7, pp. 152-167
- [11] Gautam, P. K., et al., Effect of High Temperature on Physical and Mechanical Properties of Jalore Granite, *Journal of Applied Geophysics*, 159 (2018), 6, pp. 460-474
- [12] Gautam, P. K., et al., Experimental Investigations on the Thermal Properties of Jalore Granitic Rocks for Nuclear Waste Repository, *Thermochimica Acta*, 681 (2019), 7, ID178381
- [13] Fan, L. F., et al., An Investigation of Thermal Effects on Micro-properties of Granite by X-Ray CT Technique, *Applied Thermal Engineering*, 140 (2018), 5, pp. 505-519
- [14] Yu, B. P., et al., Experimental Study on High Temperature Thermal Damage Mechanical Properties of Granite in Gonghe Basin, Qinghai, *Chinese Journal of Rock Mechanics and Engineering*, 39 (2020), 1, pp. 69-83
- [15] Kun, W., et al., Application of Nuclear Magnetic Resonance Technology in Rock Physics and Characterization of Pore Structure, *Chinese Journal of Scientific Instrument*, 41 (2020), 2, pp. 101-114

- [16] Sun, Z. G., *et al.*, Research on Thermal Damage of Beishan Granite Based on Low-Field Magnetic Resonance, *Journal of China Coal Society*, 45 (2020), 3, pp. 1081-1088
- [17] Jing, A. B., *et al.*, Influence of Different Cooling Conditions on Physical and Mechanical Properties of High Temperature Sandstone, *Rock and Soil Mechanics*, 11 (2020), 4, pp. 1-10
- [18] Gao, M. Z., *et al.*, The Location Optimum and Permeability-Enhancing Effect of a Low-Level Shield Rock Roadway, *Rock Mechanics and Rock Engineering*, 51 (2018), 9, pp. 2935-2948
- [19] Gao, M. Z., *et al.*, Mechanical Behavior of Coal under Different Mining Rates: A Case Study from Laboratory Experiments to Field Testing, *International Journal of Mining Science and Technology*, 7645 (2021), 7, pp. 78-100